

Local Conformations in the Glassy Polycarbonate of 2,2-Bis(4-hydroxyphenyl)propane (Bisphenol-A)

M. Tomaselli,^{†,‡,§} M. M. Zehnder,[‡] P. Robyr,^{||} C. Grob-Pisano,[‡]
R. R. Ernst,^{*,†} and U. W. Suter^{*,‡}

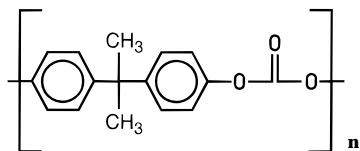
Laboratorium für Physikalische Chemie and Departement Werkstoffe, Institut für Polymere, Eidgenössische Technische Hochschule, CH-8092 Zürich, Switzerland

Received October 22, 1996; Revised Manuscript Received March 21, 1997[®]

ABSTRACT: NMR experiments were carried out on glassy samples containing ^{13}C -labeled bisphenol-A polycarbonate with isolated $\text{C}^*_{\text{carbonate}}-\text{O}-\text{C}^*_{\text{phenylene}}$ arrangements in the chains. The dihedral angle distributions in the C–O–C moieties were determined by fitting simulated spectra to the experimental data. It was found that the O–C_{phenylene} torsion angle is widely distributed with population maxima where the C–O–C plane forms an angle of ca. 55° with the phenylene ring. The carbonate units assume *trans* conformations at 135 K (torsion angle around $\text{C}^*_{\text{carbonate}}-\text{O} < 10\%$ *cis*). Three different molecular packings obtained by computer simulation with different construction methods and two different force fields yielded considerably higher *cis* contents; this discrepancy is currently still unresolved. From comparison of the data to those for single-chain models (rotational-isomeric-state models) it is concluded that considerable conformational change could be possible far below T_g .

Introduction

Following the pioneering work of Williams and Flory¹ much effort has been invested to elucidate the conformation and the local intermolecular arrangement of the glassy polycarbonate of 2,2-bis(4-hydroxyphenyl)propane (bisphenol-A polycarbonate, PC) and to determine



their relationship to the macroscopic mechanical properties.^{1–19} However, there remain many unresolved questions and a lack of conclusive experimental data on the amorphous state of the polymer.

Traditionally, the view is maintained that the chain molecules in a glass adopt similar conformations as in the melt. They are usually described as “unperturbed random coils” analogous to a system under Θ -conditions.^{20,21} In the case of polycarbonate, X-ray analysis on low molecular weight model compounds in the crystalline state^{3,8,11} and viscosity measurements of the polymer in Θ -solvents¹ indicate that the carbonate group prefers a *trans* conformation (Figure 1a), which is also supported by rotational isomeric state²¹ (RIS) calculations on the “unperturbed isolated” chain.^{1,13} This finding was called into question by various groups^{7–9,13} on the basis of the magnitude of the intramolecular interactions in a packed amorphous structure and of the low internal energy barrier of about 16 kJ/mol¹³ between the carbonate *trans*–*trans* and *cis*–*trans* (or *trans*–*cis*) states (Figure 1b), estimated from quantum-chemical and semiempirical calculations.^{9,10,13} Indeed, Hutnik et

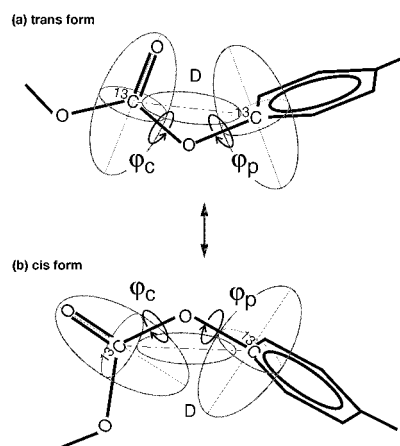


Figure 1. *Trans* (a) and *cis* (b) conformation of polycarbonate. $\varphi_c = 0^\circ$ denotes the *trans* carbonate conformation while $\varphi_c = \pm 180^\circ$ defines the *cis* state. In the planar reference conformation the phenylene dihedral angle φ_p assumes a value of zero. The relative orientations of the ^{13}C carbonyl and phenylene CSA tensors and of the dipolar coupling tensor **D** are schematically indicated for the two conformers.

al.¹³ generated atomistically detailed model structures of the polycarbonate glass and found about 28% *cis*–*trans* and 72% *trans*–*trans* carbonate conformations at 300 K, indicating that the carbonate group might be “softer” than previously assumed.

In this article we apply solid-state NMR spectroscopy²² to a selectively doubly ^{13}C -enriched polycarbonate sample to elucidate the local conformational spread at the carbonate–phenylene unit. We present evidence that the carbonate group is predominantly *trans* in the amorphous state. The orientation of the phenylene rings with respect to the carbonate group is widely distributed. We compare the NMR experiments with predictions from computational models such as the amorphous-cell approach and related methods.²³

NMR Background

A detailed discussion of the NMR procedure is given in ref 24. Here, we limit ourselves to a brief description. Two-dimensional (2D) separated local field experiments^{25,26} allow one to correlate chemical shielding

[†] Laboratorium für Physikalische Chemie.

[‡] Departement Werkstoffe.

[§] Present address: Materials Sciences Division, E.O. Lawrence Berkeley National Laboratory, 1 Cyclotron Road, Berkeley, CA 94720, and Chemistry Department, University of California, Berkeley, CA 94720.

^{||} MR Centre, Department of Physics, University of Nottingham, University Park, Nottingham NG7 2RD, England.

[®] Abstract published in *Advance ACS Abstracts*, May 1, 1997.

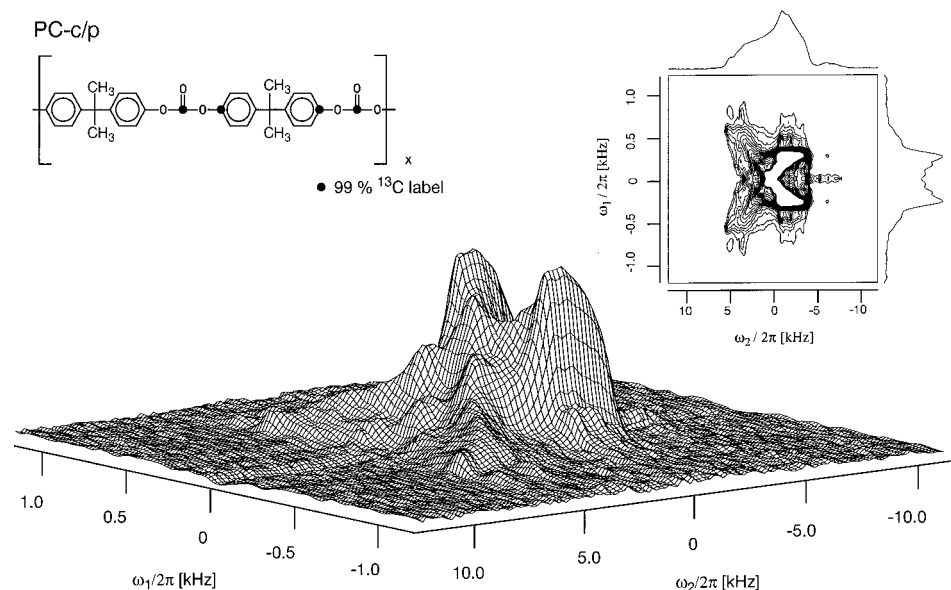


Figure 2. 2D NMR homonuclear separated local field ^{13}C spectrum of the 20% solution of doubly labeled amorphous PC-c/p (see inset, 20% doubly enriched polymer diluted in 80% natural-abundance matrix). The measurement was carried out at 135 K on a home-built spectrometer at a ^{13}C resonance frequency of 55.32 MHz (5.17 T) with a static probe assembly using nitrogen as cryogenic medium. Experimental parameters: repetition delay, 15 s; cross-polarization time, 3 ms; radiofrequency (rf) field strength, 80 kHz. Cross-polarization from the abundant proton spins is used in the preparation step of the pulse sequence. A composite π -pulse in the center of the t_1 period is applied. Amplitude modulation of the t_2 data set is achieved by a z-filter period²² before signal acquisition. On-resonance proton decoupling during t_1 and t_2 is applied. Further details of the pulse sequence are given in ref 24. The contribution from natural-abundance ^{13}C spins is eliminated by subtracting a 2D spectrum recorded for natural-abundance PC under identical experimental conditions. The spectrum is symmetrized with respect to $\omega_1 = 0$.

anisotropy (CSA) tensors with a dipole coupling tensor which can be used as an orientational reference. For carbon-13 CSA tensors a set of well-established rules has been developed for the orientation of their principal axes system (PAS) with respect to a molecule-fixed frame.^{27,28} Hence, the measurement of the correlations between CSA and dipolar tensors provides information on the orientation of isotopically labeled functional units which are indicative of the conformation of the polymer chain.

We consider the carbonate–phenylene moiety of polycarbonate with ^{13}C labels at the carbonyl and phenylene positions as shown in Figure 1. Assuming fixed bond lengths and bond angles,²¹ the relative orientation of the carbonate and phenylene ring is determined by the two torsion angles φ_c and φ_p . To determine the angular distribution functions, the experimental powder spectra are fitted by a computer simulation. For a single conformation (φ_c , φ_p) the powder spectrum is obtained by averaging over the orientational angles θ and φ that orient the magnetic field vector \mathbf{B}_0 in a molecule-fixed frame:²⁵

$$S^{\text{sc}}(\omega_1, \omega_2; \varphi_c, \varphi_p) = \frac{1}{4\pi} \int_0^\pi \sin \theta \, d\theta \int_0^{2\pi} d\varphi S^{\text{d}}(\omega_1, \omega_2; \theta, \varphi; \varphi_c, \varphi_p) \quad (1)$$

For a conformational distribution $P(\varphi_c, \varphi_p)$, the composite 2D spectrum is obtained by an integration over the distribution:

$$S^{\text{am}}(\omega_1, \omega_2) = \int_{-\pi}^\pi d\varphi_c \int_0^{\pi/2} d\varphi_p P(\varphi_c, \varphi_p) S^{\text{sc}}(\omega_1, \omega_2; \varphi_c, \varphi_p) \quad (2)$$

The distribution function $P(\varphi_c, \varphi_p)$ contains the information to be extracted from the least squares fitting procedure of the experimental 2D spectra.^{24,29}

Table 1. Principal Values of the CSA Tensors at 135 K^a

| | carbonate carbon | phenylene carbon |
|---------------------|------------------|------------------|
| δ_{11} (ppm) | 234 ± 1 | 233 ± 1 |
| δ_{22} (ppm) | 124 ± 1 | 128 ± 1 |
| δ_{33} (ppm) | 84 ± 1 | 75 ± 1 |

^a All values are given with respect to TMS.

Experiments

The measurements were carried out with bisphenol-A polycarbonate selectively enriched with ^{13}C (>99%) at the carbonate carbon and at the 4- and 4'-phenylene carbons of every second bisphenol-A residue (see Figure 2). The detailed synthesis procedure is given in ref 24. The ^{13}C -labeled polymer is characterized by $M_w = 36\,200$ and $M_w/M_n = 1.5$. A homogeneous blend of 20% ^{13}C -enriched and 80% natural-abundance polycarbonate ($M_w = 27\,500$, $M_w/M_n = 1.4$) was obtained from a 2.5% w/w solution of the polymers in dry methylene chloride by dropwise precipitation in excess heptane. The samples were annealed for 15 min at 200 °C. The assignment of the principal values of the carbonate and phenylene ^{13}C CSA tensors was performed on "singly ^{13}C -enriched" polycarbonate samples²⁴ and is given in Table 1. For the phenylene carbon the upfield principal component δ_{33}^p is associated with the normal to the ring, and the downfield value δ_{11}^p with the C–O bond direction. The most shielded axis of the carbonate CSA is perpendicular to the O–CO–O plane (δ_{33}^c) whereas the intermediate shielded axis (δ_{22}^c) is aligned with the carbonyl C=O bond direction. Small deviations ($\pm 10^\circ$) from this orientation may occur,^{24,27,28} which are, however, within the present measurement accuracy.²⁴

An experimental 2D separated local field spectrum^{25,26} of the carbonate–phenylene ^{13}C doubly-enriched polycarbonate recorded at 135 K is displayed in Figure 2. At this temperature, molecular reorientations are negligible on the time scale of the experiment.²⁴ The projection along ω_2 shows a CSA-dominated spectrum. The projection along ω_1 represents a dipolar-tensor-dominated spectrum.

The analysis proceeded stepwise. At first, to investigate the possible spread of φ_c , a composite spectrum based on a two-dimensional distribution function represented by 36 discrete

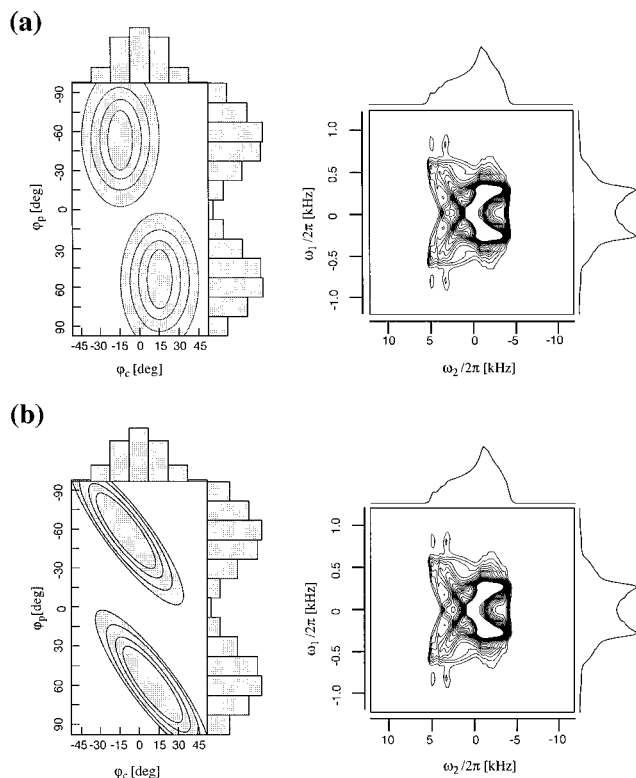


Figure 3. Fit of the 2D dihedral-angle probability distribution functions $P(\varphi_c, \varphi_p)$ based on Gaussian model functions with the corresponding computed homonuclear 2D separated local field spectra at 55 MHz ^{13}C resonance. Projections along both frequency axes are shown. In part a, uncorrelated Gaussian distributions are assumed for φ_c and φ_p (the four fit parameters, positions φ_c^0 and φ_p^0 and the variances σ_c^2 and σ_p^2 are given in Table 2). In part b, the correlation between φ_c and φ_p is allowed by including an additional tilt angle α into the Gaussian model function (see eq 3 and Table 2). The fitted distribution functions $P_C(\varphi_c, \varphi_p)$ are shown as isoprobability contour maps.

values in the interval $0^\circ < |\varphi_p| < 90^\circ$ and $-180^\circ < \varphi_c < 180^\circ$ with a resolution $\Delta\varphi_{c,p} = 30^\circ$ was fitted to the experimental spectrum. Significant population was only detected for the *trans* carbonate state ($\varphi_c = 0^\circ \pm 45^\circ$) with a negligible contribution ($< 5\%$) from the *cis* carbonate isomer ($90^\circ \geq |\varphi_c| \leq 180^\circ$). Consequently, consideration of φ_c was restricted in subsequent evaluations to the interval $-50^\circ < \varphi_c < 50^\circ$. In order to keep the number of fit parameters low, the dihedral-angle probability distribution function $P(\varphi_c, \varphi_p)$ was approximated by a bivariate Gaussian function fitted in the interval $-50^\circ < \varphi_c < 50^\circ$ and $0^\circ \leq |\varphi_p| \leq 90^\circ$:

$$P_C(\varphi_c, \varphi_p) = \frac{1}{2\pi\sigma_1\sigma_2} \times \exp\left(-\frac{[(\cos\alpha)(\varphi_p - \varphi_p^0) - (\sin\alpha)(\varphi_c - \varphi_c^0)]^2}{2\sigma_1^2}\right) \times \exp\left(-\frac{[(\sin\alpha)(\varphi_p - \varphi_p^0) + (\cos\alpha)(\varphi_c - \varphi_c^0)]^2}{2\sigma_2^2}\right) \quad (3)$$

The two centroids φ_c^0 and φ_p^0 and the variances σ_1^2 and σ_2^2 define four fit parameters. The 'tilt angle' α gives the orientation of the axes of the bivariate Gaussian function with respect to the φ_p axis and allows for a possible correlation of both dihedral angles. If a constraint of $\alpha = \pi/2$ is applied, then $\sigma_1 = \sigma_c$ and $\sigma_2 = \sigma_p$. Two fitted Gaussian distribution functions $P_C(\varphi_c, \varphi_p)$ together with the corresponding theoretical spectra are displayed in Figure 3. For the fit in Figure 3a, α is constrained at 90° , while, in Figure 3b, α is used as a free fit parameter. The extracted parameters for $P_C(\varphi_c, \varphi_p)$ are

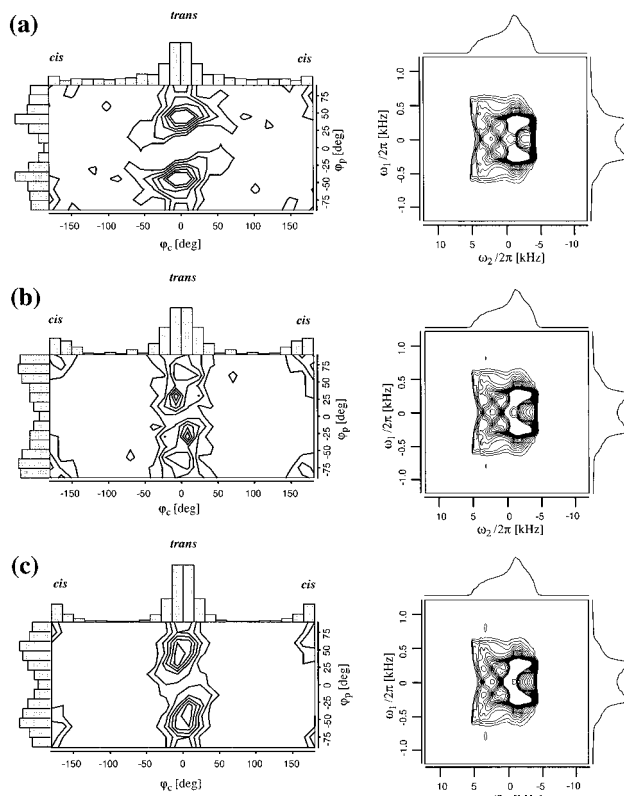


Figure 4. Carbonate-phenylene dihedral angle probability distribution functions $P(\varphi_c, \varphi_p)$ together with the calculated 2D separated local field spectra (see eq 2) derived from three sets of computer-generated dense amorphous microstructures. (a) 13 microstructures with a degree of polymerization $x = 35$ ($M = 4532$, box edge length = 18.44 Å) and two structures with $x = 151$ ($M = 19\,264$, box edge length = 29.87 Å) were analyzed.¹³ Bond lengths and bond angles are fixed in the model, and an ad hoc force field was used. The packings were created using the "amorphous-cell" algorithm.²³ Goodness-of-fit criterion of the simulated spectrum: $\chi^2 = 2.13$ (relative to the normalized minimum χ^2 of Table 2). Setting a limit of $|\varphi_c| = 90^\circ$ to separate *trans* from *cis*, the relative fraction of carbonate *cis* states amounts to $f_{cis} = 0.28$. (b) Two microstructures with a degree of polymerization $x = 137$ ($M = 17\,576$, box edge length = 29.15 Å). An all-atoms force field with flexible geometry (pcff91³¹) was employed, and the packings were obtained by a "condensation-from-the-gas-phase" MD procedure.³⁰ $\chi^2 = 1.75$, $f_{cis} = 0.3$. (c) Three microstructures with a degree of polymerization $x = 150$ ($M = 19\,014$, box edge length = 29.74 Å). The same force field as in part b was used, but the packings were constructed with an "amorphous-cell" algorithm, different from part a, and followed by MD annealing.³² $\chi^2 = 1.5$, $f_{cis} = 0.25$.

given in Table 2 with the relative 'goodness of fit criterion' (the minimum χ^2 -value is normalized to 1). The 'tilted Gaussian model' gives a slightly better fit to the experimental spectrum. A numerical evaluation (based on an F-test with a confidence coefficient $q = 0.1$) suggests that the preference of the Gaussian model with a tilt angle $\alpha = 55^\circ \pm 20^\circ$ is significant.²⁴

Computer Simulations

The experimentally obtained dihedral-angle distribution functions can be compared to the results of computer-simulated model structures of glassy polycarbonate. Three different sets of microstructures, computed in a different context, were evaluated, leading to the dihedral-angle distributions for φ_c and φ_p shown in Figure 4: (a) The distribution results from 15 minimum energy structures with rigid bond lengths and bond angles obtained by Hutnik et al.,¹³ based on an ad hoc force

Table 2. Gaussian Fits at 135 K

| parameters | tilt angle constrained | tilt angle optimized |
|--|---------------------------|-------------------------|
| tilt angle α (deg) ^a | 90 | 55 ± 20 |
| maximum φ_p^0 (deg) | -54 ± 20 | -57 ± 10 |
| maximum φ_c^0 (deg) | -11 ± 10 | -7 ± 8 |
| width σ_p (deg) | 26 ± 10 | |
| width σ_c (deg) | 14 ± 5 | |
| width σ_1 (deg) ^b | | 31 ± 10 |
| width σ_2 (deg) ^b | | 5 ± 2 |
| χ^2 (arb unit) | 1.05 | 1 |

^a The angle α is defined with respect to the φ_p axis. ^b σ_1 and σ_2 are given in the tilted frame of reference.

field. (b) The distribution represents two snapshot microstructures obtained from a constant-stress molecular dynamics (MD) procedure.³⁰ The amorphous structures were generated by densification from the gas phase using the unconstrained Cartesian-coordinate force field pcff91.³¹ (c) Three microstructures obtained from an amorphous-cell procedure followed by a molecular dynamics "annealing" procedure using the unconstrained pcff91 force field lead to the distribution shown.³²

The theoretical separated local field spectra calculated from the simulated distribution functions $P(\varphi_c, \varphi_p)$ with eq 2 are displayed in the right frames of Figure 4. The goodness-of-fit criterion χ^2 for the three simulated spectra is given in the caption of Figure 4 and can be compared with the values given in Table 2. The microstructure ensemble (a) gives the worst agreement ($\chi^2 = 2.13$) with the experimental spectrum due to the wide scatter of carbonate conformations with high intramolecular energy. The other two sets of microstructures, with smaller width of the "trans-trans" peak and smaller fraction of *cis-trans* carbonate rotamers (setting a limit of $|\varphi_c| = 90^\circ$ to separate *trans* from *cis*) show better agreement with the experimental spectrum ($\chi^2 = 1.5$ –1.75). All simulated phenylene-dihedral angle distribution functions (see projections onto φ_p in Figure 4) are in agreement with the experimental findings. No significant correlation of the phenylene ring orientation and the *trans* carbonate conformation is observed in these glass models.

Discussion

The NMR experiments show that for glassy polycarbonate at 135 K the carbonate group is predominantly in the planar *trans* form, in agreement with the conformation found in the crystalline low-molecular-weight analogues.^{3,8,11} On the basis of an error analysis, we deduce that less than 10% of all carbonate groups are in a *cis* conformation.²⁴ Neither at 135 K nor at 300 K²⁴ have any changes in the line shapes of the static 1D and 2D spectra been observed over the entire period of measurements of several months. The orientation of the phenylene rings with respect to the carbonate units is disordered. The analysis according to both Gaussian models reveals a population maximum at $\varphi_p \approx 55^\circ$, in agreement with the results of Erman et al.³ and corroborating previous expectations based on quantum-chemical and empirical force-field calculations.¹³ The 'tilted Gaussian model' seems to indicate a weak correlation between φ_p and φ_c , although no firm conclusion can be drawn due to the limited experimental resolution: A deviation of the carbonate unit from the *trans* geometry results in a correlated tilt of the neighboring phenylene rings such that the carbonate and phenylene planes remain at approximately unchanged

orientations. This behavior was suggested earlier by Sundararajan⁶ on the basis of an analysis of the intramolecular-energy surface of the fragment considered (steric hindrance between the carbonyl oxygen and the ortho C–H of the phenylene rings competing with the π -electron delocalization of the *trans* carbonate-phenylene fragment). The experimentally extracted dihedral-angle distribution functions are in agreement with the RIS analysis for polycarbonate.^{1,13} The single-chain models estimate a relative carbonate *cis-trans* content of less than 5% at 135 K and one of less than 10% at 300 K (relative to *trans-trans*).

In contrast to this finding, all amorphous-cell microstructures, although obtained with three different simulation protocols and two different force fields,^{13,30,32} predict a typical *cis-trans* content of 25–30%. Two different reasons might account for this deviation: One reason might be found in the fact that the simulations are based on an unphysical spatially periodic continuation condition with a characteristic length of 20 Å where finite-size effects imposed by the system dimensions could enforce the presence of high-energy carbonate conformations. Since a variation of the cell dimensions in simulations is not practical over a sufficiently large range, this suspicion cannot be confirmed at present. Another reason for the deviation of the models might be the fact that all microstructures have been "created" at a temperature of ca. 300 K. It is implicitly assumed that, below the glass transition temperature T_g , *cis-trans* isomerization in glassy polycarbonate is virtually impossible and that the models, therefore, represent a state of "frozen-in liquid disorder" near T_g . This view is at variance with assumptions of several other authors, based on theoretical and experimental studies: Substantial intramolecular chain dynamics for polycarbonate below T_g has been proposed before by Jones,⁷ implying a Hall-Helfand³³ type of correlated conformational *cis-trans* isomerization which retains the *cis* content but allows for "migration" of *cis* conformations and their annihilation at the chain end. Henrichs et al.^{4,11} argued that the carbonate movement is tied to the motion of the phenylene rings, such that a distortion of the carbonate unit from the planar *trans-trans* conformation facilitates π -phenylene ring flipping,^{34–37} whereas Yee and co-workers,^{2,16–17} on the basis of dynamic mechanical relaxation experiments, even concluded that significant intramolecular cooperative motion extending to about seven repeat units is active below T_g .

The conformational analysis of PC, presented in this paper, shows that at 135 K the *cis-trans* population is significantly lower than the RIS estimate of 20–25% at the annealing temperature of 470 K indicates. This implies that even 265 K below T_g (450 K) structural rearrangements at the carbonate-phenylene unit might take place such that the local thermodynamic equilibrium in the glass can be approached. More work is needed to gain a satisfactory understanding of these observations.

Acknowledgment. We acknowledge support by the Swiss National Foundation of Science. We thank Marcel Utz for valuable discussions.

References and Notes

- (1) Williams, A. D.; Flory, P. J. *J. Polym. Sci., Polym. Phys. Ed.* **1968**, *6*, 1945–1952.
- (2) Yee, A. F.; Smith, S. A. *Macromolecules* **1981**, *14*, 54–64.

- (3) Erman, B.; Marvin, D. C.; Irvine, P. A.; Flory, P. J. *Macromolecules* **1982**, *15*, 664–669. Erman, B.; Wu, D.; Irvine, P. A.; Marvin, D. C.; Flory, P. J. *Macromolecules* **1982**, *15*, 670–673.
- (4) Henrichs, P. M.; Linder, M.; Hewitt, J. M.; Massa, D.; Isaacson, H. V. *Macromolecules* **1984**, *17*, 2412–2416.
- (5) Schaefer, J.; Stejskal, E. O.; Perchak, D.; Skolnick, J.; Yaris, R. *Macromolecules* **1985**, *18*, 368–373.
- (6) Sundararajan, P. R. *Can. J. Chem.* **1985**, *63*, 103–110.
- (7) Jones, A. A. *Macromolecules* **1985**, *18*, 902–906.
- (8) Perez, S.; Scaringe, R. P. *Macromolecules* **1987**, *20*, 68–77.
- (9) Bicerano, J.; Clark, H. A. *Macromolecules* **1988**, *21*, 585–597.
- (10) Laskowski, B. C.; Yoon, D.; McLean, D.; Jaffe, R. L. *Macromolecules* **1988**, *21*, 1629–1633.
- (11) Henrichs, P. M.; Luss, H.; Scaringe, R. P. *Macromolecules* **1989**, *22*, 2731–2742.
- (12) Henrichs, P. M.; Nicely, V. A. *Macromolecules* **1990**, *23*, 3193–3194.
- (13) Hutnik, M.; Argon, A. S.; Suter, U. W. *Macromolecules* **1991**, *24*, 5956–5961. Hutnik, M.; Gentile, F. T.; Ludovice, P. J.; Suter, U. W.; Argon, A. S. *Macromolecules* **1991**, *24*, 5962–5969. Hutnik, M.; Argon, A. S.; Suter, U. W. *Macromolecules* **1991**, *24*, 5970–5979.
- (14) Lee, P. L.; Schaefer, J. *Macromolecules* **1992**, *25*, 5559–5560.
- (15) Lamers, C.; Schärpf, O.; Schweika, W.; Batoulis, J.; Sommer, K.; Richter, D. *Physica B* **1992**, *180 & 181*, 515–518.
- (16) Jho, J. Y.; Yee, A. F. *Macromolecules* **1991**, *24*, 1905–1913.
- (17) Xiao, C.; Yee, A. F. *Macromolecules* **1992**, *25*, 6800–6809.
- (18) Schmidt, A.; Kowalewski, T.; Schaefer, J. *Macromolecules* **1993**, *26*, 1729–1733.
- (19) Lee, P. L.; Schaefer, J. *Macromolecules* **1995**, *28*, 1921–1924. Lee, P. L.; Kowalewski, T.; Poliks, M. D.; Schaefer, J. *Macromolecules* **1995**, *28*, 2476–2482.
- (20) Flory, P. J. *Principles of Polymer Chemistry*; Cornell University Press: Ithaca, NY, 1953.
- (21) Flory, P. J. *Statistical Mechanics of Chain Molecules*, reprinted ed.; Hanser Verlag: Munich, 1989.
- (22) Ernst, R. R.; Bodenhausen, G.; Wokaun, A. *Principles of Nuclear Magnetic Resonance in One and Two Dimensions*; Clarendon Press: Oxford, 1987.
- (23) Theodorou, N.; Suter, U. W. *Macromolecules* **1985**, *18*, 1467–1478.
- (24) Tomaselli, M.; Robyr, P.; Meier, B. H.; Grob-Pisano, C.; Ernst, R. R.; Suter, U. W. *Mol. Phys.* **1996**, *89*, 1663–1694.
- (25) Linder, M.; Höhener, A.; Ernst, R. R. *J. Chem. Phys.* **1980**, *73*, 4959–4970.
- (26) Nakai, T.; McDowell, C. A. *Chem. Phys. Lett.* **1994**, *217*, 234–238.
- (27) Veeman, W. S. *Prog. Nucl. Magn. Reson. Spectrosc.* **1984**, *16*, 193–235.
- (28) Mehring, M. *Principles of High Resolution NMR in Solids*; Springer Verlag: Berlin, 1983.
- (29) Hagemeyer, A.; Brombacher, L.; Schmidt-Rohr, K.; Spiess, H. W. *Chem. Phys. Lett.* **1990**, *167*, 583–587.
- (30) Gusev, A. A.; Zehnder, M. M.; Suter, U. W. *Macromolecules* **1994**, *27*, 615–616.
- (31) Maple, J. R.; Hwang, M.-J.; Stockfisch, T. P.; Dinur, U.; Waldmann, M.; Ewig, C. S.; Hagler, A. T. *J. Comput. Chem.* **1994**, *15*, 162–182.
- (32) Tiller, A.; Gusev, A. A.; Suter, U. W. In preparation.
- (33) Hall, C. K.; Helfand, E. J. *J. Chem. Phys.* **1982**, *77*, 3275–3282.
- (34) Spiess, H. W. *J. Mol. Struct.* **1983**, *111*, 119–133. Spiess, H. W. *Colloid Polym. Sci.* **1983**, *261*, 193–209.
- (35) Roy, A. K.; Jones, A. A.; Inglefield, P. T. *Macromolecules* **1986**, *19*, 1356–1362.
- (36) Schaefer, J.; Stejskal, E. O.; McKay, R. A.; Dixon, W. T. *Macromolecules* **1984**, *17*, 1479–1489.
- (37) Hansen, M. T.; Blümich, B.; Boeffel, C.; Spiess, H. W.; Morbitzer, L.; Zembrod, A. *Macromolecules* **1992**, *25*, 5542–5544.

MA961565B